analytical chemistry

pubs.acs.org/ac

Review

Nanozyme-Enabled Analytical Chemistry

Sirong Li,[§] Yihong Zhang,[§] Quan Wang,[§] Anqi Lin,[§] and Hui Wei*

Cite This: *Anal. Chem.* 2022, 94, 312−323

Read Online

ACCESS | Metrics & More | Article Recommendations | Supporting Information

CONTENTS

In 2007, landmark research recognized ferromagnetic nanoparticles (Fe_3O_4 NPs) as the substitute of horseradish peroxidase (HRP) for their alike catalytic ability to oxidize signal molecule 3,3′,5,5′-tetramethylbenzidine (TMB) during the classical enzyme linked immunosorbent assay (ELISA).[1] Shortly, Wei and Wang constructed a cascade assay with glucose oxidase (GOx) and Fe_3O_4 NPs to monitor the concentration of glucose, demonstrating the feasibility of coupling an enzyme and inorganic nanoparticles for cascade biosensing.[2] From then on, a growing number of nanomaterials (such as carbon,[3−5] metal,[6−8] metal oxide,[9−11] metal−organic frameworks,[12−14] and others[15−18]) have been demonstrated with different enzyme-like activities and now are collectively termed as nanozymes by integrating the two concepts of nanomaterial and enzymes.[19−26] Notably, compared with conventional nanocatalysts, nanozymes emphasize mimicking the function of enzymes which convert substrates under physiological conditions. For other artificial enzymes, nanozymes stress the scaffold of nanomaterials, enriching the discipline of artificial enzymes from organic chemistry[27] into inorganic chemistry and even their interpenetration. Moreover, the repertoires of nanomaterials, such as economic cost, high stability, and multifunctional physicochemical properties, precisely overcome the intrinsic instability and cost of enzymes and, in the meantime, offer more potential in rational design and functionalization, such as magnetic response, photothermal properties,[28] surface enhanced Raman scattering (SERS),[29] fluorescence,[30] etc. The above multifunctionality not only provides possibilities for environmental protection and healthcare treatment but also conducts multiplatform based sensing and imaging.

From 2007 to now, thousands of research papers have been published in the field of nanozymes. Since the landmark nanozyme was discovered in classical ELISA, it is necessary to summarize subsequent progress in analytical chemistry and to further advance the nanozyme research. As illustrated in Scheme 1, nanozymes with peroxidase-like activity and oxidase-like activity can be employed in conducting sensing arrays. In principle, higher activity lowers the limit of detection (LOD), while better selectivity excludes other interferences, providing a solid foundation for analytical applications. Therefore, the strategies to conduct high performance nanozymes (enhanced activity and specificity) will be discussed first. Then, miscellaneous analytes both *in vitro* and *in vivo* are discussed. Further, nanozyme assisted diagnostic imaging technology is also covered. In the final section, we discussed the current challenges that the field of nanozymes faces in the hope that researchers provide more efforts to fulfill those gaps.

NANOZYMES WITH HIGHER ACTIVITY

One of the distinct features of enzymes are their ultrahigh reaction rate. Correspondingly, nanozymes with comparable or even superior activity are long-standing pursuits. Two strategies are discussed here to improve the activity of nanozymes: (1) increasing the inherent activity by delicate

Special Issue: Fundamental and Applied Reviews in Analytical Chemistry 2022

Published: December 6, 2021

https://doi.org/10.1021/acs.analchem.1c04492
Anal. Chem. 2022, 94, 312−323

Scheme 1. Schematic Illustration of Nanozyme-Based Sensing Platforms[a]

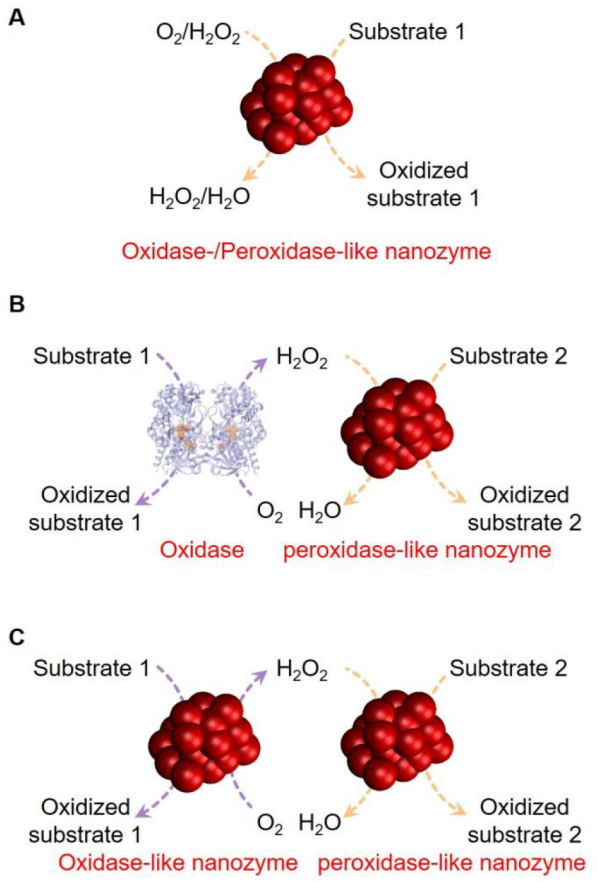

[a](A) Sole nanozyme-based sensing platform by utilizing the oxidase-/peroxidase-like activity. (B) Cascade sensing array with natural oxidase and peroxidase-like nanozyme. (C) Cascade sensing array with oxidase-like nanozyme and peroxidase-like nanozyme. Various signals with colorimetric, chemiluminescent, fluorometric, and SERS response can be obtained when applying relevant substrates.

design and (2) boosting the activity by confinement effect or external stimulators.

Improving the Inherent Activity of Nanozymes. By embedding a hemin-like Fe−N_4 active site into graphene (Fe−N-rGO), a 700-fold improvement was achieved compared to the parent graphene.[31] Another record high catalytic efficiency of peroxidase-like enzymes was reported by Xia and his collaborators.[32] The catalytic constant (k_{cat}) of the Ni−Pt nanozyme is 10^4 times higher than that of natural peroxidases. Immune detection of carcinoembryonic antigen (CEA) was employed to manifest the advantage of the Ni−Pt nanozyme (Figure 1A). The boosted activity of Ni−Pt achieved an ultrasensitive LOD of 1.1 pg/mL, which is hundreds of times lower than the traditional enzyme-based and pure Pt nanozyme-based ELISAs (Figure 1B and C).

Also, numerous inspiring studies developed other effective strategies to prepare high performance nanozymes even though they have not been used for analysis. We discussed some representative studies here owing to instructive insights and their potential application in analytical chemistry. For instance, instead of incorporating the identical active site of enzymes (Fe−N_4) in single-atom material, a FeN_3P-centerd single-atom nanozyme (FeN_3P-SAzyme) from the metal−organic framework (MOF) template was fabricated and demonstrated superior peroxidase-like activity to that of natural counterparts.[33] Similarly, a series of MIL-53 (Fe) with different substituents on the ligands were investigated to imitate the secondary coordination environment modulation of enzymes[12]. Finally, oxidase-like activity was found linearly enhanced by a growing electron-withdrawing ability. The density functional theory (DFT) calculation revealed a Hammett-type structure activity linear free energy relationship (H-SALR) in those MIL-53 (Fe) nanozymes. The greater the value of the Hammett σ_m is, the higher the oxidase-like activity of nanozymes that can be obtained. Additionally, MOF, metals, and metal oxides are also suitable systems for structure−activity relationship studies. The peroxidase-like activity of perovskite transition metal oxides (ABO_3) can be predicted by the descriptor of e_g.[34] What is more, having benefited from the booming development of computation, a universal descriptor (energy) was identified to screen peroxidase-like nanozymes.[35] This ab initio calculation strategy not only avoided screening material dependent descriptors but also systematically predicted the peroxidase-like activity of nanomaterials, revealing the versatility of computer-aided design.

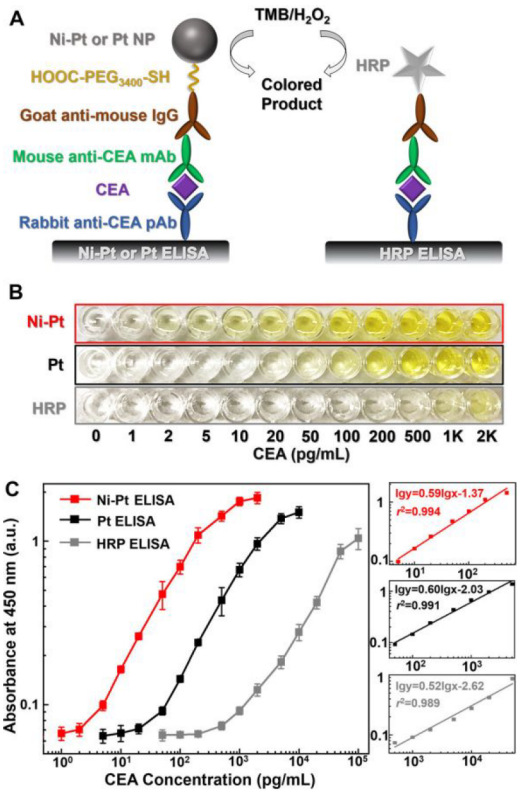

Figure 1. Ni−Pt nanozyme-based ELISA and its improved performance. (A) Schematics of the three ELISAs of CEA. (B) Representative photographs taken from the ELISAs of CEA standards. (C) Corresponding calibration curves (left) along with linear range regions (right) of the detection results in B. Error bars indicate standard deviations of eight independent measurements. Reprinted with permission from ref 32. Copyright 2021 American Chemical Society.

Acquired Activity of Nanozymes. Strategies to acquire the activity of nanozymes are summarized into two parts: (1) utilizing the nanostructure of nanozymes as the framework to mimic the subcellular compartments, which is also termed as the confinement effect in catalysis science; (2) taking physical

https://doi.org/10.1021/acs.analchem.1c04492
Anal. Chem. 2022, 94, 312−323

factors (such as light) as a promoter or enhancer to activate the activity.

MOFs have been viewed as an ideal host to embed guests because of their high crystallinity and porosity.[36] On the basis of the distinct features of MOFs, GOx and peroxidase-like hemin were assembled within ZIF-8 (zeolitic imidazolate framework) to construct an integrated nanozyme (INAzyme), see Figure 2A.[37] The nanoscale ZIF-8 cages raised the contact

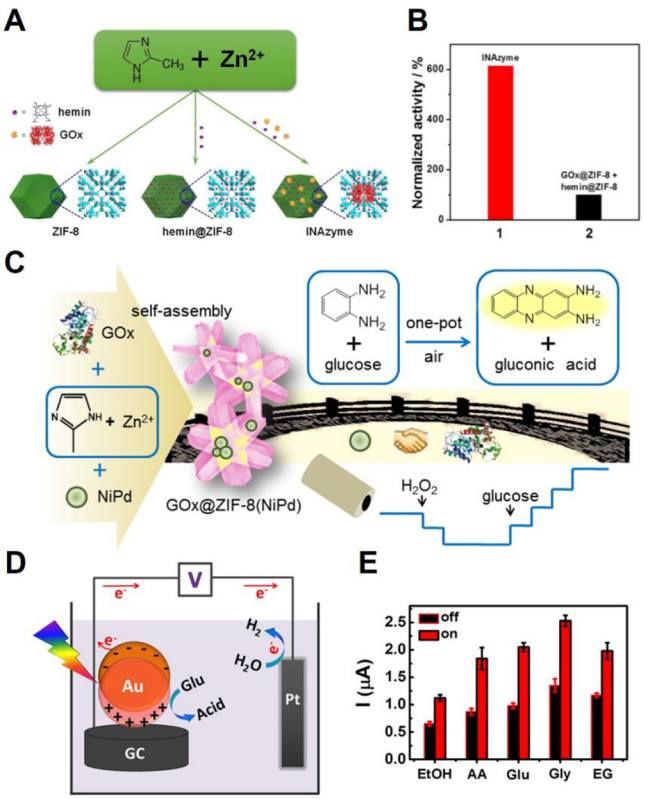

Figure 2. Acquired activity of nanozymes. (A) Schematic illustration of the biocompatible one-step synthetic approaches to nanoscaled ZIF-8 and ZIF-8-based nanozymes in aqueous solution at room temperature. (B) Normalized cascade catalytic activity of the INAzyme (1) and the mixture of hemin@ZIF-8 and GOx@ZIF-8 (2). (C) Schematic illustration of the GOx@ZIF-8(NiPd) nanoflower for tandem catalysis. (D) Illustration of the electrochemical setup and the principle of plasmon-accelerated electrochemical reaction (PAER). (E) Generality of the proposed PAER mechanism toward different electrochemical reactions. A and B reprinted with permission from ref 37. Copyright 2016 American Chemical Society. C reprinted with permission from ref 39. Copyright 2017 John Wiley and Sons. D and E reprinted with permission from ref 40. Copyright 2017 American Chemical Society.

possibility between the substrate and enzymes by reducing the mass diffusion barrier and minimizing the active intermediate loss, accordingly reaching a 6-fold enhancement in catalytic efficiency (Figure 2B). In addition, the INAzyme had good stability after 2 months of storage. Benefiting from the above advantages of INAzyme, Wei et al. successfully conducted a real-time platform to monitor the dynamic changes of striatum glucose in living rats' brains. Encouraged by the above success, a similar platform was subsequently conducted to measure glucose and lactate in living tissues through the INAzyme of AuNPs@MIL-101@oxidase.[38] The detection was carried out by making use of the plasmonic and biocatalytic properties of AuNPs. The H_2O_2 generated from oxidase would oxidize the Raman-inactive reporter leucomalachite green into the active malachite green (MG) by peroxidase-like AuNPs. Therefore, a SERS signal for monitoring the concentration of glucose and lactate was generated. On the basis of this, the INAzyme was used to evaluate the therapeutic efficacy of astaxanthin (ATX) in living rats' cerebral ischemic injury model. Besides sensing *in vivo*, a tandem nanozyme GOx@ZIF(NiPd) was also successfully demonstrated for monitoring glucose *in vitro* (Figure 2C),[39] suggesting the universal improvement for analysis both *in vitro* and *in vivo*.

Due to the environmentally friendly and noninvasive properties of light, it has been widely investigated in optogenetics, healthcare, energy transformation, and catalysis. Similar to the promoter and enhancer in biological systems, light responsive nanozymes can also turn on or off their activity with or without the irradiation of light. Noble metals are classic plasmonic materials. In addition to the boosted photocatalysis of AuNPs, the electrochemical reaction of AuNPs to oxidize glucose like a GOx can also be accelerated upon localized surface plasmon resonance (Figure 2D).[40] However, the versatile oxidation toward ethanol (EtOH), ascorbic acid (AA), glucose (Glu), glycerol (Gly), and ethylene glycol (EG) in Figure 2E indicates the challenge of specificity.

NANOZYMES WITH BETTER SPECIFICITY

As discussed above, another distinct challenge that is in great demand to solve is the specificity of nanozymes. Herein, two strategies are summarized on the recent progress.

Improving the Inherent Specificity of Nanozymes. For most reported oxidase-like nanozymes, i.e., ceria and noble metals, peroxidase- and catalase-like activities are exhibited. Though those nanozymes function as a catalase in a neutral or alkaline environment, the optimized activity of oxidase and that of peroxidase are extremely close. On the one hand, the biactivity yields an inevitable background signal, decreasing the detection sensitivity. On the other hand, it leaves a dilemma that the majority of nanozyme-based cascade arrays still cannot skip the usage of oxidases if discrimination toward homologues is expected. Namely, such enzyme−nanozyme cascade arrays still suffer the inherent drawbacks of enzymes. To tackle the above challenges, a catechol oxidase-like MOF-818 was developed by replicating the copper center in natural catechol oxidases (Figure 3A).[41] Because of the similar active sites, both the MOF-818 and catechol oxidase can oxidize phenol substrates (i.e., 3,5-di-*tert*-butylcatechol, 3,5-DTBC) and meanwhile reduce O_2 to peroxide (Figure 3B) but fail to oxidize nonphenol substrates (i.e., TMB, as shown in Figure 3C) either with or without the presence of H_2O_2, manifesting the negligible peroxidase-like activity and a good substrate selectivity toward phenols. Owing to such excellent specificity, two different sensing platforms can be established for detecting H_2O_2 in Figure 3D and detecting 2,4-dichlorophenol (2,4-DP) in Figure 3E.

In addition to learning from nature, classical material engineering strategies also enhanced the desired specificity of nanozymes. For example, by selectively doping the specified heteroatom nitrogen (N) into reduced graphene oxide (rGO), a carbon-nanozyme with sole peroxidase-like activity was obtained, leading to a better linear range for sensing of H_2O_2 than pristine rGO.[42] Additionally, molecular imprinted polymers (MIPs), which are also described as chemical antibodies, were coated on the surface of nanozymes, resulting

https://doi.org/10.1021/acs.analchem.1c04492
Anal. Chem. 2022, 94, 312−323

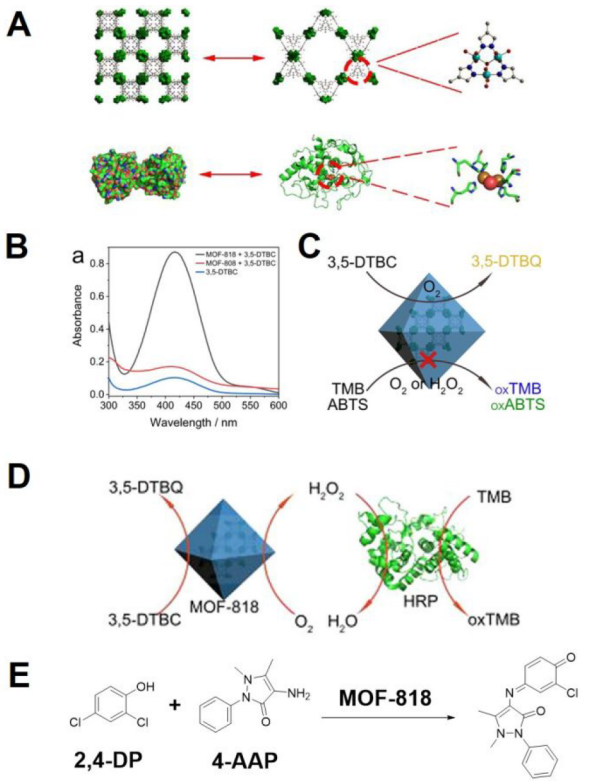

Figure 3. Design and catalytic performance of catechol oxidase-like MOF-818. (A) Catechol oxidase (PDB code 1BT1) inspired MOF-818 nanozyme. (B) UV−vis absorption spectra of 3,5-DTBC in the absence and presence of 50 μg/mL MOF-818 or MOF-808. (C) Schematic illustration on the selective oxidizing of 3,5-DTBC by MOF-818. (D) Scheme of detecting H_2O_2. (E) Reaction of 2,4-DP and 4-aminoantipyrine (4-AAP) catalyzed by MOF-818. Reprinted with permission from ref 41. Copyright 2020 American Chemical Society.

in a 100-fold improvement in specificity.[43] Further, supramolecular units as well as an external stimulator (light) assisted the nanozyme core to recognize chiral monosaccharides and selectively oxidize the *L*-configurable monosaccharides only.[44]

The unrivaled efficiency and specificity of enzymes are derived from their sophisticated, hierarchical structure, namely the primary and secondary coordination environment, delicate tunnel/geometry for substrates, and the assistance from cofactors/coenzymes. In contrast, too little is known to realize such an advanced structure within a molecule or a nanoparticle. Recently, mechanical bonds were first adopted in the covalent organic framework (COF) to mimic the dynamic conjugation change during the reaction pathway of organophosphorase.[45] Novel adventures and substantial efforts are on the way to create comparable and even superior enzyme mimics.

Acquired Specificity of Nanozymes. Even though MIPs endow the desired recognition in nanozyme systems, each of the substrates requires a customized modification approach for the variety of templates. Further, the thickness of the MIP coating may inversely hinder the direct interaction between substrates and active sites exposed on the surface. To avoid these disadvantages, the cross-reactive sensor array stands out, as it recognizes various analytes by increasing the signal channels and discriminates between them after proper data processing (such as linear discrimination analysis, LDA).[46−48] By fully utilizing multiple dimensions of output signals (deriving from either the greater number of nanozymes or the multifunctionality of nanozymes), accordingly, cross-reactive sensor arrays not only save time-consuming specific modification but also reserve the advantages of nanozymes in facile preparation, low cost, and strong adaptability.

Such enzyme-free cross-reactive sensor arrays have been verified among a variety of analytes, such as metal ions,[49] bioactive small molecules,[50,51] cells,[48,52] etc. In a seminal work, different nanozymes (i.e., Pt, Ru, and Ir in Figure 4A) were employed with *o*-phenylenediamine (OPD) as a chromogenic substrate.[48] Due to the distinct response of each noble metal toward biological thiols, proteins, and cancer cells, the nanozyme cross-reactive sensor array is capable of analyzing unknown samples and real samples with universality and accuracy. In addition to utilizing the discriminated activity of nanozymes, the multiple absorption peaks of the Au frame nanoparticles and chromogenic substrate TMB (A_{370}, A_{450}, and A_{650}) can also be applied as LDA arrays.[52] More interestingly, benefiting from the modular design of MOFs, structurally engineered MOFs with enhanced selectively were developed to distinguish six different antioxidants (glutathione, GSH; mercaptosuccinic acid, MA; thioglycolic acid, TA; cysteine, Cys; ascorbic acid, AA; gallic acid, GA). By varying modulators during synthesis, MOFs with different morphologies were obtained (3D, 2D, and dendritic-like MOFs in Figure 4B),[53] resulting in variation of pore size. Finally, a single MOF with 2D structure and dendritic structure (AD-TCPP) can distinguish six antioxidants separately, as in Figure 4C. Also, light is introduced to activate and enhance the oxidase-like activity of the as-prepared MOFs, thereby achieving dual enhancement in both the activity and selectivity.

NANOZYME-ENABLED ANALYTICAL CHEMISTRY *IN VITRO*

So far, nanozyme-enabled detection covers various targets ranging from small molecules,[51,54−56] ions[57−61] to macromolecules,[62−67] cells,[68,69] and microorganisms.[70−75] And, these versatile *in vitro* detection targets are summarized in Table S1. Because of the limitation of space, we took the multifunctional nanozyme-enabled *in vitro* detection, nanozyme powered strips/devices, and newly emerged drug analysis as examples to illustrate recent developments in nanozyme-enabled analytical chemistry *in vitro*.

Multifunctional Nanozyme-Enabled *in Vitro* Detection. In our previous review,[76] we summarized two representative multifunctional nanozymes with magnetic properties (iron based nanozymes) in detection, separation, enrichment and enhancement, and surface plasmon resonance (noble metal nanozymes) in enhanced sensing platforms. Thus, we complemented photothermally featured nanozymes for thermometer detection here.

The photothermal effect has been widely studied in noninvasive tumor treatment. Coincidentally, the classical photothermally active materials, such as Prussian blue[77] and noble metals,[78,79] also showed prominent enzyme-like activity, indicating a bridge to link a thermal signal to enzyme activity. Prussian blue NPs were first utilized as a photothermal probe in immunoassays to give out a heat signal, which was detected by a thermometer.[77] Then, as displayed in Figure 5A, the DNA hybridization induced aggregation of AuNPs can convert the specific DNA binding into heat. Therefore, a quick response was visualized, and the polymerase chain reaction (PCR) free

https://doi.org/10.1021/acs.analchem.1c04492
Anal. Chem. 2022, 94, 312−323

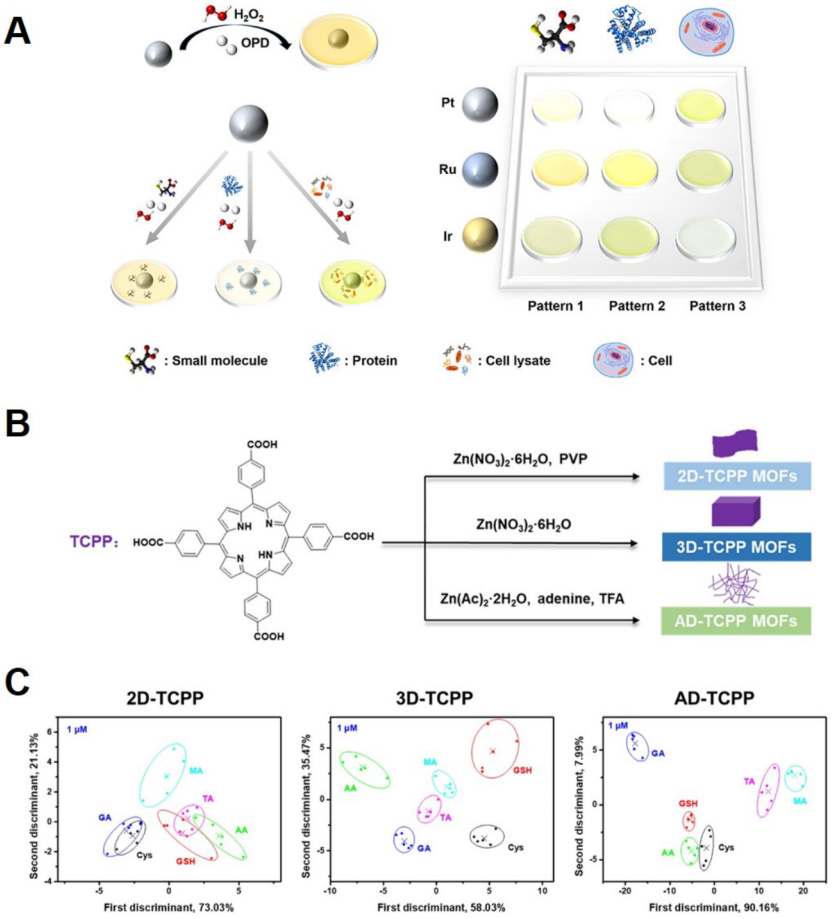

Figure 4. Nanozyme-based cross-reactive sensor array. (A) Nanozyme sensor arrays for detecting versatile analytes. (B) Synthesis procedures of 2D-TCPP, 3D-TCPP, and AD-TCPP. (C) 2D-TCPP (left), 3D-TCPP (middle), and AD-TCPP (right) sensor arrays for discriminations against 1 μM of antioxidants. A reprinted with permission from ref 48. Copyright 2018 American Chemical Society. B and C reprinted with permission from ref 53. Copyright 2019 American Chemical Society.

genetic detection technique was developed by using common thermometers with AuNPs with a sensitivity up to 0.28 nM.[79] Subsequent research constructed an aggregation-activated oxidase mimic AuNP@β-CD (Figure 5B) to detect the Hg^{2+} ions in blood samples.[60] During the detection, the oxidase-like activity of AuNP@β-CD could be activated once Hg^{2+} existed. Then, the oxidized TMB yielded heat under the irradiation of a laser. The concentration dependent absorbance spectrum in Figure 5C and D corresponds well with the temperature changes in Figure 5E and F. Considering the noninvasive characteristic of light, it is promising to develop such photothermal featured biosensing for *in vivo* detection.

Nanozyme Powered Strips/Devices. One of the distinct features of nanozymes that can be afforded is relatively higher stability or higher tolerance in processing and storage. Herein, nanozyme powered strips and devices are introduced.

The global pandemic of severe acute respiratory syndrome coronavirus 2 (SARS-CoV-2) is a major public concern. Therefore, developing a fast, accurate, and facile approach to detect SARS-CoV-2 is crucial to controlling epidemic spread. As shown in Figure 6A, Yan and co-workers built a sensitive and rapid paper test platform, utilizing nanozyme powered chemiluminescence.[75] With the optimized antibody toward spike-receptor binding domain (S-RBD) protein, they achieved a similar detection limit of SARS-CoV-2 antigen (360 $TCID_{50}$/mL in Figure 6B, by chemiluminescence paper and 360 $TCID_{50}$/mL in Figure 6D, by ELISA) and wider detection range (360 $TCID_{50}$/mL to 1.14 × 10^3 $TCID_{50}$/mL, by chemiluminescence paper and from 360 to 2850 $TCID_{50}$/mL, by ELISA). Moreover, the strips recognized pseudo-SARS-CoV-2 specifically, while the commercial influenza A antigen testing kits failed (Figure 6E).

Choi and co-workers also established a microfluidic device (Figure 6F and 6G) to quantify H_2O_2 and glucose in real time in which the metal-free nanozyme, K^+ modified graphitic carbon nitride performed good oxidase- and peroxidase-like activities.[80] As shown in Figure 6G, the microfluidic device was irradiated first to oxidize glucose and generate H_2O_2 with near 100% quantum efficiency. Then, in the dark, this bifunctional mimic can catalyze H_2O_2 to oxidize chromogenic substrate gradually with the increase of glucose and finally achieving a good linear response.

Additionally, point of care testing (POCT) devices are also explored with nanozymes. Li and co-workers used a glucose meter as a platform to detect different size substrates ranging from molecules to proteins (Figure 6H).[81] Electrochemical measurements with lateral flow immune strips gave sensitive and accurate results for the detection of disease biomarkers.

Nanozyme-Enabled Drug Analysis. In the majority of analytical applications of nanozymes, the higher activity is primarily considered as it directly correlates with a higher conversion rate. However, few works focus on the brake, i.e.,

https://doi.org/10.1021/acs.analchem.1c04492
Anal. Chem. 2022, 94, 312−323

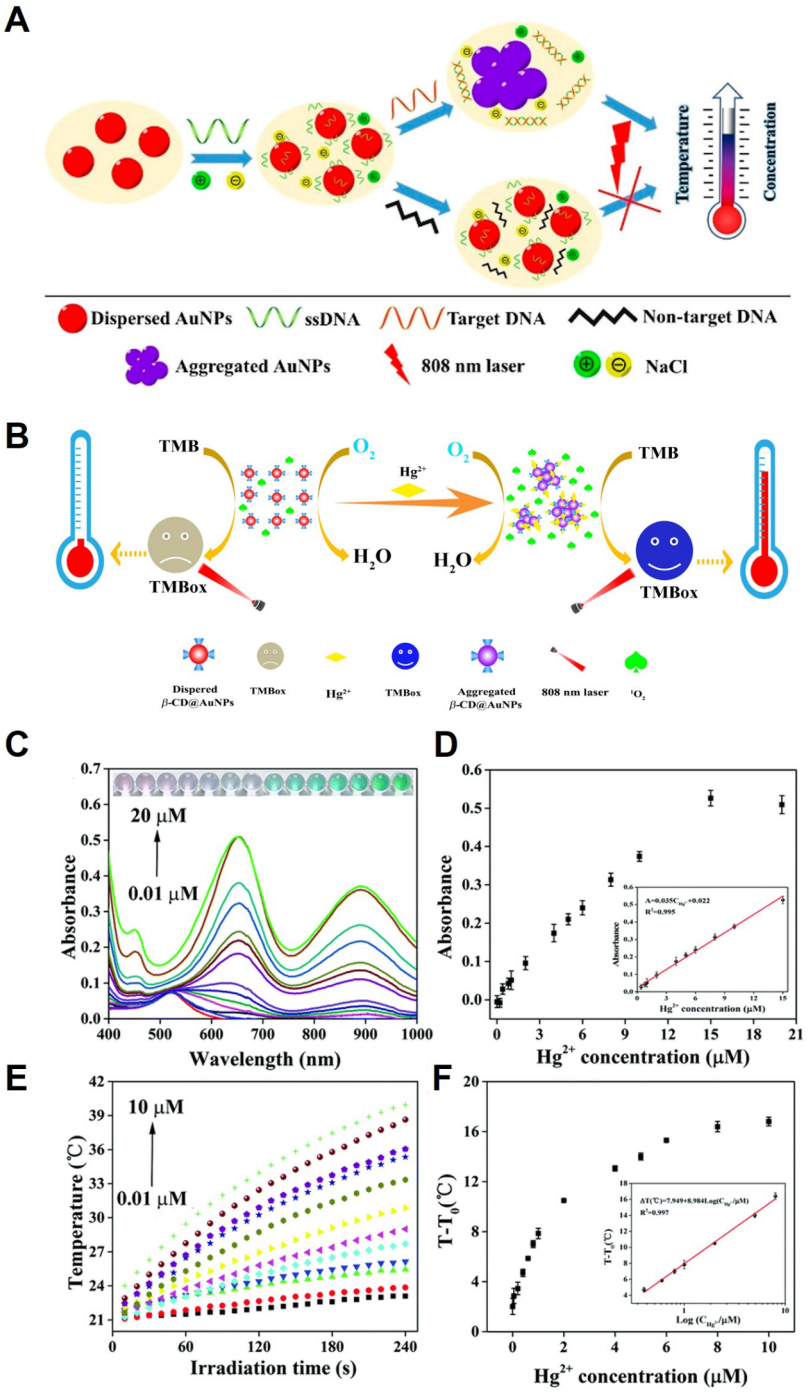

Figure 5. Multifunctional nanozyme-enabled assays. (A) Schematic illustration of the principle of AuNP aggregation-induced photothermal biosensing of target DNA using a thermometer. (B) Schematic of the AuNP@β-CD aggregation-based photothermometric platform for the Hg^{2+} analysis. (C) Vis−NIR spectra and (E) temperature of the proposed sensing systems upon different Hg^{2+} concentrations (inset: photos of the corresponding solution color). The corresponding plot of (D) absorbance changes at 652 nm (A_{652}) and (F) temperature increase (ΔT) versus the concentration of Hg^{2+} (inset: the corresponding linear-fitted lines of Hg^{2+}). A reprinted with permission from ref 79. Copyright 2020 American Chemical Society. B−F reprinted with permission from ref 60. Copyright 2020 Royal Society of Chemistry.

termination of enzymatic reaction which also contributes to signal pathways with negative feedback. Recently, a Fe−N−C nanozyme was reported to resemble the cytochrome P450 (CYP) with both accelerated and inhibited activity.[82] Owing to the precise copy of Fe−N centered coordination within carbon, the as-prepared Fe−N−C nanozyme exhibited similar inhibition behavior and close IC_{50} with CYP3A4 after the treatment of ketoconazole (Figure 7A). More inhibitors were employed in Figure 7B. Strikingly, neither erythromycin, the inhibitor of 3-hydroxy-3-methylglutaryl coenzyme A (HMG-CoA), nor enoxacin, the inhibitor of CYP1A2, showed prominent inhibition toward the Fe−N−C nanozyme relative to that of ketoconazole and grapefruit juice. Both the identical activity of converting 1,4-dihydropyridine (1,4-DHP) and the similar inhibition behavior by ketoconazole confirmed the structure and function resemblance between CYP1A2 and Fe−

https://doi.org/10.1021/acs.analchem.1c04492
Anal. Chem. 2022, 94, 312−323

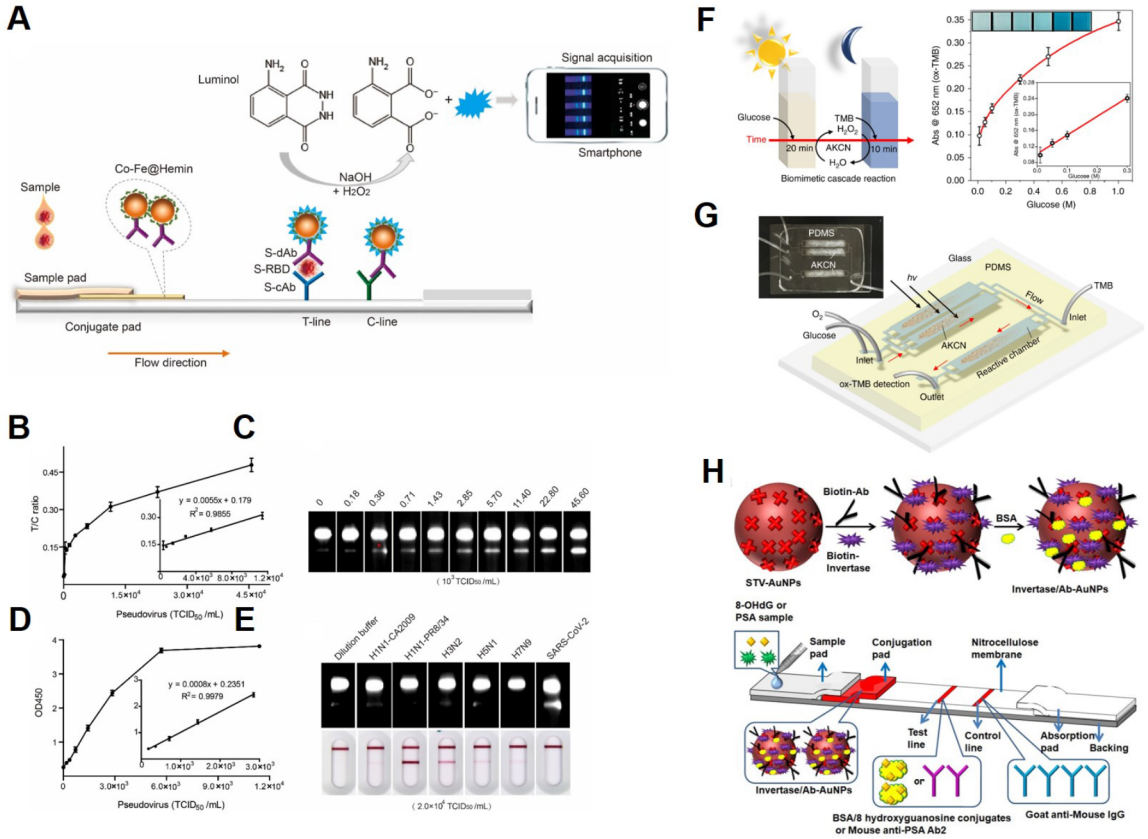

Figure 6. Nanozyme powered strips and devices. (A) Schematic illustration of the nanozyme chemiluminescence paper test for SARS-CoV-2 S-RBD antigen. (B) Calibration curve of pseudovirus test. (C) Gradient detection of pseudo-SARS-CoV-2 samples using nanozyme chemiluminescence test paper. (D) ELISA detection of the pseudo-SARS-CoV-2 samples. (E) Nanozyme chemiluminescence strip specifically recognized the pseudo-SARS-CoV-2. The inactivated samples of H1N1, H3N2, H5N1, and H7N9 with the same titer were tested positively using the commercial Influenza A antigen testing kits. (F) Left: scheme of the cascade reaction with continuous O_2-purging in a batch mode. Right: the concentration−response curve with the linear calibration plots (inset) and color change (inset) for glucose detection in the batch reactor. (G) Scheme of the cascade reaction in a microfluidic device and actual device image (inset). (H) Design of test strips for quantitative detection of 8-hydroxy-2′-deoxyguanosine (8-OHdG) or prostate specific antigen (PSA). A−E reprinted with permission from ref 75. Copyright 2021 Elsevier. F and G reprinted with permission from ref 80. Copyright 2019 Springer Nature. H reprinted with permission from ref 81. Copyright 2019 Elsevier.

N−C nanozymes. It is hoped that such nanozymes will substitute CYP1A2 in accessing the interaction between drugs and therefore decreasing part of the cost during drug discovery.

NANOZYME-ENABLED ANALYTICAL CHEMISTRY *IN VIVO*

***In Vivo* Sensing Platforms.** Previously, an INAzyme-based platform was demonstrated to monitor the dynamic changes of glucose and lactose in living brain or tissues benefiting by the enhanced activity.[38] Subsequently, a self-cascade nanozyme (V_2O_5) was conducted to achieve a nonenzymatic online optical detection platform (OODP).[83] Specifically, the as-prepared V_2O_5 can mimic dual enzyme-like activity (GOx and peroxidase) which can couple into tandem reactions for glucose sensing (Figure 8A). As demonstrated in Figure 8B, three components, artificial cerebrospinal fluid (aCSF), V_2O_5, and TMB, were pumped and reacted in order. Then, the color change of TMB was recorded by an objective lens-based optical detector which monitored the dynamic change of glucose through light intensity profile. Apart from glucose, H_2S, a critical neuromodulator in the central nervous system, has also been exploited by using a similar online optical detection platform based on Prussian blue analog nanocubes (PBA NCs).[84] What is more, an online electrochemical platform was further developed by Lin to detect 3,4-dihydroxyphenylacetic acid in living brains.[85]

Of note, such nanozyme-enabled studies in living systems provide an additional opportunity to investigate the function of organisms/signal molecules and also shed insights into the bioeffects of nanoparticle based biosensors.

***In Vivo* Diagnosis and Imaging.** Nanozymes with magnetic properties have been widely studied as magnetic resonance imaging (MRI) probes.[86−88] However, to highlight the characteristics of nanozymes versus common nanomaterials, we here discussed mainly the cases utilizing the enzyme-like activity instead of other physical features. Since the generation and consumption of reactive oxygen species (ROS) are found to be closely related to metabolism and illness, ROS related nanozymes with catalase-, peroxidase-, and oxidase-like activities are all proved helpful for *in vivo* diagnosis and imaging.

The catalase-like nanozyme is capable of generating O_2 bubbles with the presence of H_2O_2, which is overaccumulated around tumors or inflamed tissues. By utilizing the generated bubbles, the ultrasound (US) signal can be enhanced and thus realize a stronger contrast in tumor[89] (Figure 9A) or inflamed tissues.[90]

https://doi.org/10.1021/acs.analchem.1c04492
Anal. Chem. 2022, 94, 312−323

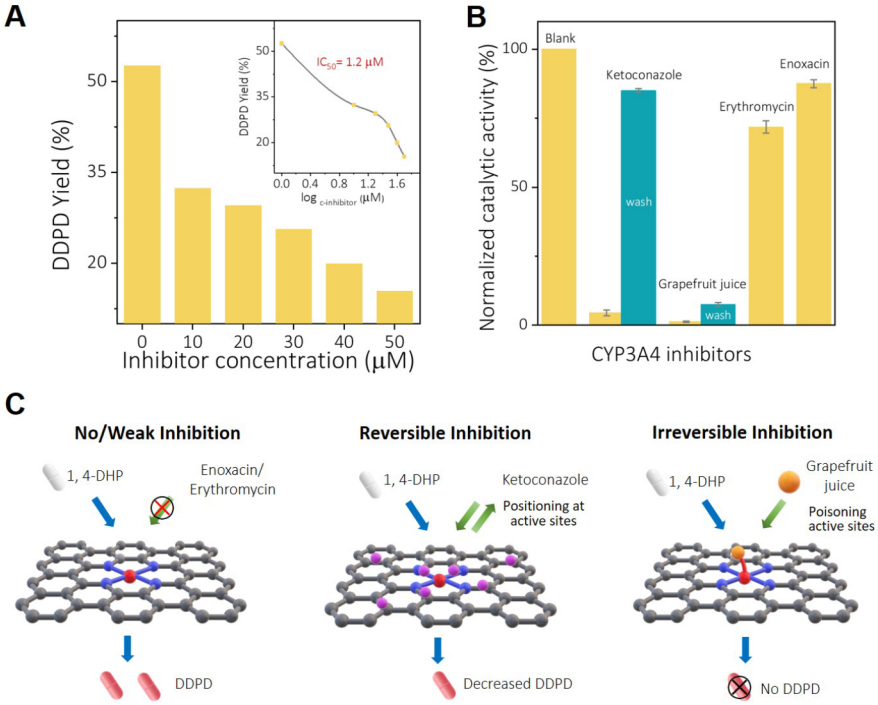

Figure 7. CYP3A4-like inhibition behaviors and mechanism of Fe−N−C. (A) Metabolization of 1,4-DHP by Fe−N−C with different concentrations of ketoconazole inhibitor. Inset: the logarithmic transformation in calculating IC_{50}. (B) Normalized catalytic activity with different inhibitors: ketoconazole (60 μM), grapefruit juice supernatant (a dose of 1 mL), erythromycin (60 μM), and enoxacin (60 μM). Blank sample stands for 200 μM of 1,4-DHP catalyzed by 50 mg/mL Fe−N−C-400 without any inhibitors in 1 mL of aqueous solution. The deactivated Fe−N−C-400 was recycled by washing it with water and was retested without any inhibitors. (C) The possible mechanism for no/weak reversible and irreversible inhibition. Reprinted with permission from ref 82. Copyright 2020 John Wiley and Sons.

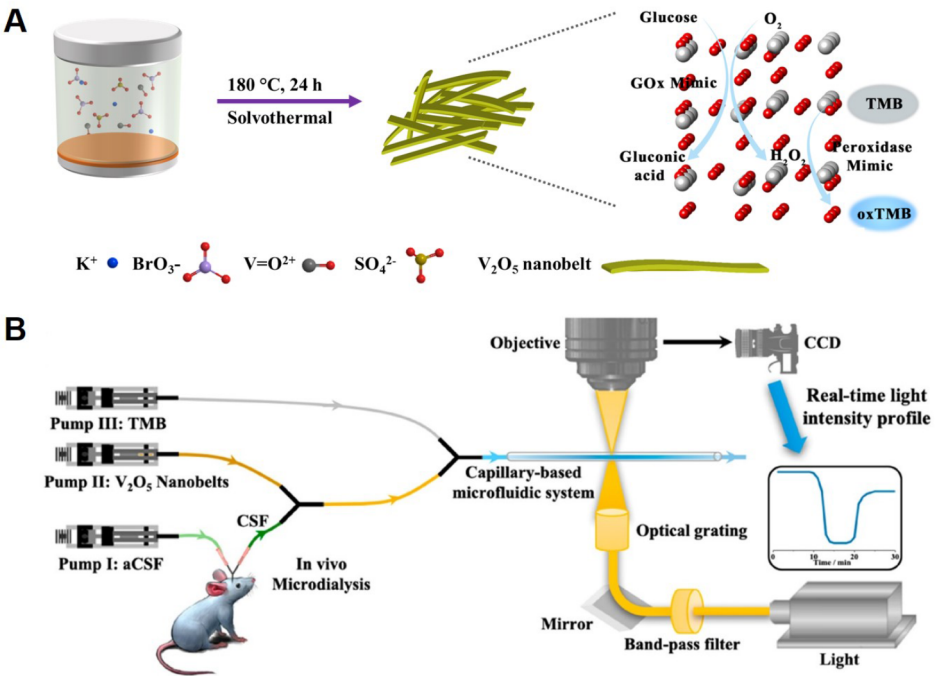

Figure 8. Nanozyme-enabled assays in living brains. (A) Synthesis and tandem catalytic process of V_2O_5 nanobelts. (B) Online optical detection platform by directly integrating a visible light absorption-based probe generated by the cascade catalysis from V_2O_5 nanobelts with a homemade capillary-based microfluidic system. Reprinted with permission from ref 83. Copyright 2020 American Chemical Society.

In vivo colorimetric diagnosis of tumors by peroxidase-like gold nanoclusters (AuNCs, around 2 nm) was realized through passive targeting based on the enhanced permeability and retention (EPR) effect.[8] As illustrated in Figure 9B−D, the peptide linker between AuNCs and biotin would be cleaved when protease (i.e., metalloproteinase 9, MMP9, a specific

https://doi.org/10.1021/acs.analchem.1c04492
Anal. Chem. 2022, 94, 312−323

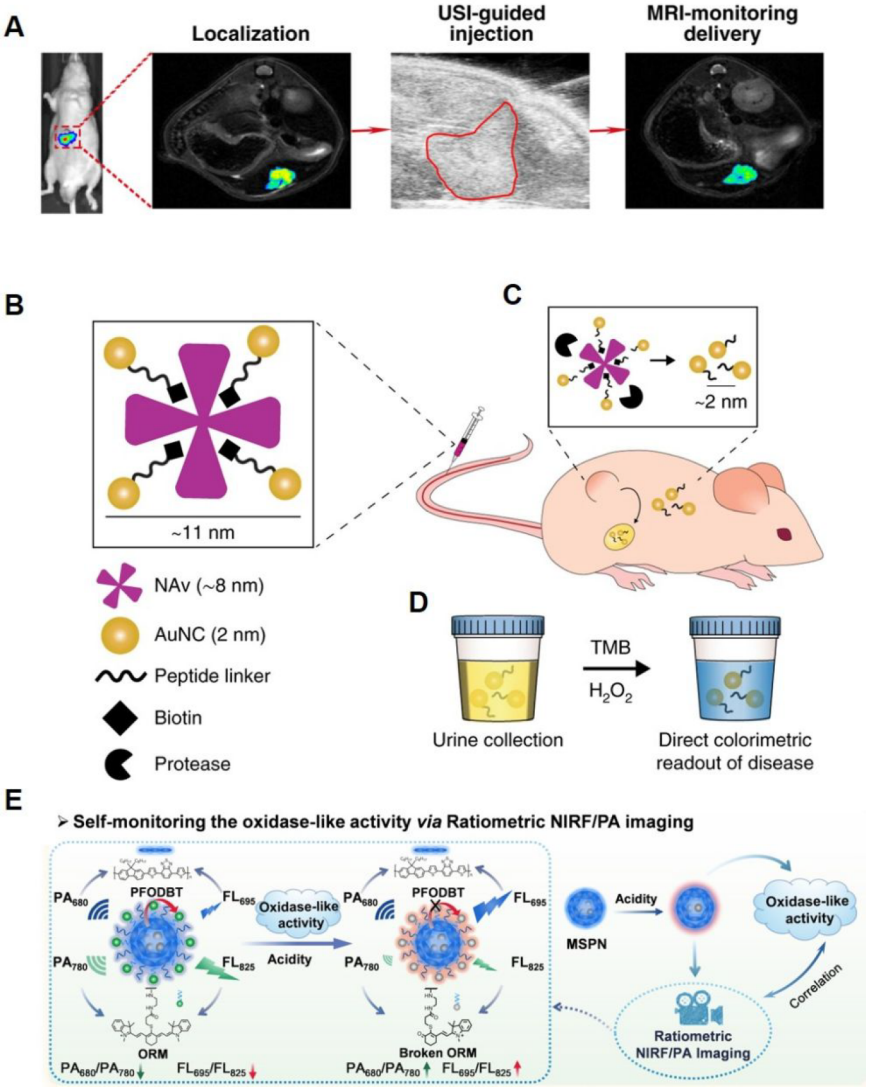

Figure 9. Nanozyme-enabled *in vivo* diagnosis and imaging. (A) Orthotopic hepatocellular carcinoma (HCC) model verified and multimodality imaging-guided encapsulin-produced magnetic iron oxide nanocomposites (eMION) delivery. (B) Catalytic AuNCs were conjugated to a neutravidin (NAv) protein scaffold through a biotinylated protease-cleavable peptide linker. (C) The protease-sensitive AuNC−NAv complex (~11 nm) designed to specifically disassemble when exposed to the activity of the relevant dysregulated proteases at the site of disease was injected i.v. After protease cleavage (top), the liberated AuNCs (~2 nm) were filtered through the kidneys and into urine. (D) The AuNCs were detected in the cleared urine by measuring their ability to oxidize TMB in the presence of H_2O_2 and generate a colored signal that can be easily read by the eye. (E) The schematic illustration of MSPN for ratiometric NIRF-PA imaging of the oxidase-like activity. A reprinted with permission from ref 89. Copyright 2020 Springer Nature. B−D reproduced with permission from ref 8. Copyright 2019 Springer Nature. E reprinted with permission from ref 10. Copyright 2021 John Wiley and Sons.

protease in cardiovascular disease or cancer) is overexpressed. Once disassembled, the ultrasmall AuNCs would be efficiently cleared by the kidneys via urine. With the addition of H_2O_2 and TMB, the disassembled AuNCs could yield a colorimetric readout by its peroxidase-like activity. A 13-fold enhancement was observed within 1 h in colorectal cancer rats compared to health groups, offering a reliable and facile method for early diagnosis.

Very recently, Song *et al.* reported a ratiometric nanozyme platform for predicting tumor therapeutic effects by detecting the acid-dependent oxidase-like activity of manganese-semiconducting polymer-based oxidase-like nanozyme (MSPN).[10] In particular, oxidase-responsive molecule (ORM) was conjugated with the semiconducting polymer (PFODBT). Once the oxidase-like activity is activated by acidic microenvironment around tumor, ORM would be oxidized, resulting in the effective fluorescence resonance energy transfer (FRET) between PFODBT (emission at 695 nm) and ORM (emission at 825 nm). Therefore, the ratio of FL_{695}/FL_{825} and photoacoustic (PA) ratiometric signal PA_{680}/PA_{780} increased (Figure 9E). Further, the oxidase-like activity would also generate ROS to kill cancer cells. Accordingly, the recovered tumor is sure to alleviate the acidic microenvironment and further inhibit the oxidase-like activity, leading to decreased signals from two channels. Hence, the good relevance between therapeutic effects and ratiometric near-infrared fluorescent (NIRF)-PA signaled nanozyme activity is promising in the future to guide clinical, precise cancer treatment and evaluate therapeutic outcomes.

https://doi.org/10.1021/acs.analchem.1c04492
Anal. Chem. 2022, 94, 312−323

CONCLUSIONS AND PERSPECTIVES

Since the date when the first case applied Fe_3O_4 NPs to substitute the peroxidase in commercial ELISA, nanozymes started creating a picture of an elegant blueprint for cheaper but more stable enzyme analogs. More than a decade past, the blueprint of nanozymes, thought to be finished, still showed us the remarkable establishment achieved. In this Review, we concentrated on the substantial efforts that nanozymes made in analytical chemistry. First of all, the prosperous development in catalysis science, materials chemistry, and computation contributes to advancing nanozymes with higher activity, which is the prerequisite for nanozymes to replace enzymes or surpass enzymes. With some record high activity that nanozymes reported, the lack of specificity becomes prominent, as it may be interfered with by analogues and thus hinder a real enzyme-free cascade sensing array. Chemical recognition such with as MIPs and supramolecular chemistry and multichannel based fingerprint-like recognition were introduced into the nanozyme world. More importantly, emerging materials, such as single-atom carbon,[91] MOF,[92] and COF[45] with adaptive bonds, also exhibited enormous potential to delicately imitate nature. Such high performance nanozymes, together with their multifunctionality, depict the versatile analytical targets and analytical approaches that nanozymes can reach, from *in vitro* sensing and drug assessment to *in vivo* detection, diagnosis, and imaging. However, as a developing field, despite the inspiring efforts achieved, it is still necessary and instructive to discuss here the demanding challenges of such a young field, in regard to clearing the gap between nanozymes and enzymes and trying to give a hint on the direction to pursue subsequent efforts.

Mechanism Studies of Nanozymes. Even though a similar Michaelis−Menten constant can be derived from the Michaelis−Menten kinetic equation, it is still difficult to obtain the true TOF of a nanozyme for the problem to measure the exact number of active sites with a single particle.[26] Additionally, more and more evidence suggests that the mechanism for nanozymes not only depends on the category of materials but also relies on the substrates, leading to a more complicated situation.[93] Only the combination of experimental data and deeper mechanism study can better guide researchers to screen nanozymes with good activity and better specificity.

Commercial Products with Nanozymes. As discussed in the beginning, two of the distinct features of nanozymes are their stability and ease of processing. Applying nanozymes inside devices not only can make full use of the multifunctionalities of nanozymes (i.e., conductivity) but also extend the life-cycle of enzyme based biosensors. However, few commercial nanozyme-powered strips or portable devices have come to the market. Ongoing progress is remarkably encouraged to make a deep understanding of nanozymes both in mechanisms and in practical applications.

The nanozymes are the cross products of artificial enzymes and nanomaterials. However, investigating the inherent enzyme-like activity of nanomaterials (especially inorganic nanomaterials) may not only aid a cheaper, more stable, or faster detection approach but also shed light on the origin of life since catalytic minerals must have arisen prior to primitive life.

ASSOCIATED CONTENT

Supporting Information

The Supporting Information is available free of charge at https://pubs.acs.org/doi/10.1021/acs.analchem.1c04492.

Summary of *in vitro* detection targets in the most recent two years (PDF)

AUTHOR INFORMATION

Corresponding Author

Hui Wei − *Department of Biomedical Engineering, College of Engineering and Applied Sciences, Nanjing National Laboratory of Microstructures, Jiangsu Key Laboratory of Artificial Functional Materials, Nanjing University, Nanjing, Jiangsu 210023, China; State Key Laboratory of Analytical Chemistry for Life Science, School of Chemistry and Chemical Engineering, Chemistry and Biomedicine Innovation Center (ChemBIC), Nanjing University, Nanjing, Jiangsu 210023, China*; orcid.org/0000-0003-0870-7142; Email: weihui@nju.edu.cn

Authors

Sirong Li − *Department of Biomedical Engineering, College of Engineering and Applied Sciences, Nanjing National Laboratory of Microstructures, Jiangsu Key Laboratory of Artificial Functional Materials, Nanjing University, Nanjing, Jiangsu 210023, China*

Yihong Zhang − *State Key Laboratory of Analytical Chemistry for Life Science, School of Chemistry and Chemical Engineering, Chemistry and Biomedicine Innovation Center (ChemBIC), Nanjing University, Nanjing, Jiangsu 210023, China*

Quan Wang − *Department of Biomedical Engineering, College of Engineering and Applied Sciences, Nanjing National Laboratory of Microstructures, Jiangsu Key Laboratory of Artificial Functional Materials, Nanjing University, Nanjing, Jiangsu 210023, China*

Anqi Lin − *Department of Biomedical Engineering, College of Engineering and Applied Sciences, Nanjing National Laboratory of Microstructures, Jiangsu Key Laboratory of Artificial Functional Materials, Nanjing University, Nanjing, Jiangsu 210023, China*

Complete contact information is available at: https://pubs.acs.org/10.1021/acs.analchem.1c04492

Author Contributions

[§]Authors contributed equally.

Notes

The authors declare no competing financial interest.

Biographies

Sirong Li achieved her Ph.D. degree in the College of Engineering and Applied Sciences at Nanjing University in 2021. She received her B.E. degree from Tianjin University in 2016 and carried out undergraduate research under the supervision of Professor Wenxin Wang at University College Dublin. During her Ph.D. program training in Professor Hui Wei's group, she explored hydrolytic nanozymes, such as data-informed hydrolytic nanozyme design and their biomedical applications.

Yihong Zhang is a Ph.D. candidate in the College of Engineering and Applied Sciences at Nanjing University. After he received his B.S. degree from Lanzhou University in 2018, he joined Professor Hui

https://doi.org/10.1021/acs.analchem.1c04492
Anal. Chem. 2022, 94, 312−323

Wei's group to start his research journey. Currently, his research interest is synthesis and the application of nanozymes.

Quan Wang is a Ph.D. candidate in the College of Engineering and Applied Sciences at Nanjing University. After he received his B.S. degree from Wuhan University in 2017; he joined Professor Hui Wei's group to start his research journey. Now, his research interests focus on the rational design of nanozymes and discovery of their potential applications.

Anqi Lin is a Ph.D. candidate in the College of Engineering and Applied Sciences at Nanjing University. After she received her B.S. degree from Nanjing University in 2018, she joined Professor Hui Wei's group to start her research journey. Now her research interests focus on the rational design of nanozymes and their biomedical applications.

Hui Wei is a Professor at Nanjing University and a Fellow of the Royal Society of Chemistry. He received his B.S. degree from Nanjing University (advisor: Professor Xinghua Xia) and Ph.D. degree from Changchun Institute of Applied Chemistry, Chinese Academy of Sciences (advisor: Professor Erkang Wang). He then joined Professors Yi Lu's and Shuming Nie's groups for two Post-doctoral trainings before he started his independent career at Nanjing University. His research interests are focused on the design and synthesis of functional nanomaterials (such as nanozymes) and the development of new methodologies for analytical and biomedical applications.

■ ACKNOWLEDGMENTS

This work was supported by National Natural Science Foundation of China (21874067 and 21722503), the National Key R&D Program of China (2019YFA0709200), CAS Interdisciplinary Innovation Team (JCTD-2020-08), PAPD Program, and Fundamental Research Funds for the Central Universities (021314380195).

■ REFERENCES

(1) Gao, L.; Zhuang, J.; Nie, L.; Zhang, J.; Zhang, Y.; Gu, N.; Wang, T.; Feng, J.; Yang, D.; Perrett, S.; Yan, X. *Nat. Nanotechnol.* **2007**, *2*, 577−583.
(2) Wei, H.; Wang, E. *Anal. Chem.* **2008**, *80*, 2250−2254.
(3) Song, Y.; Qu, K.; Zhao, C.; Ren, J.; Qu, X. *Adv. Mater.* **2010**, *22*, 2206−2210.
(4) Xi, J.; Zhang, R.; Wang, L.; Xu, W.; Liang, Q.; Li, J.; Jiang, J.; Yang, Y.; Yan, X.; Fan, K.; Gao, L. *Adv. Funct. Mater.* **2021**, *31*, 2007130.
(5) Li, F.; Li, S.; Guo, X.; Dong, Y.; Yao, C.; Liu, Y.; Song, Y.; Tan, X.; Gao, L.; Yang, D. *Angew. Chem., Int. Ed.* **2020**, *59*, 11087−11092.
(6) Cao-Milán, R.; Gopalakrishnan, S.; He, L. D.; Huang, R.; Wang, L.-S.; Castellanos, L.; Luther, D. C.; Landis, R. F.; Makabenta, J. M. V.; Li, C.-H.; Zhang, X.; Scaletti, F.; Vachet, R. W.; Rotello, V. M. *Chem.* **2020**, *6*, 1113−1124.
(7) Gao, F.; Shao, T.; Yu, Y.; Xiong, Y.; Yang, L. *Nat. Commun.* **2021**, *12*, 1−18.
(8) Loynachan, C. N.; Soleimany, A. P.; Dudani, J. S.; Lin, Y.; Najer, A.; Bekdemir, A.; Chen, Q.; Bhatia, S. N.; Stevens, M. M. *Nat. Nanotechnol.* **2019**, *14*, 883−890.
(9) Weng, Q.; Sun, H.; Fang, C.; Xia, F.; Liao, H.; Lee, J.; Wang, J.; Xie, A.; Ren, J.; Guo, X.; Li, F.; Yang, B.; Ling, D. *Nat. Commun.* **2021**, *12*, 1−14.
(10) Teng, L.; Han, X.; Liu, Y.; Lu, C.; Yin, B.; Huan, S.; Yin, X.; Zhang, X. B.; Song, G. *Angew. Chem., Int. Ed.* **2021**, *60*, 26142−26150, DOI: 10.1002/anie.202110427.
(11) Huo, M.; Wang, L.; Chen, Y.; Shi, J. *Nat. Commun.* **2017**, *8*, 357.
(12) Wu, J.; Wang, Z.; Jin, X.; Zhang, S.; Li, T.; Zhang, Y.; Xing, H.; Yu, Y.; Zhang, H.; Gao, X.; Wei, H. *Adv. Mater.* **2021**, *33*, 2005024.
(13) Luo, H. B.; Castro, A. J.; Wasson, M. C.; Flores, W.; Farha, O. K.; Liu, Y. *ACS Catal.* **2021**, *11*, 1424−1429.
(14) Feng, D.; Gu, Z.; Li, J.; Jiang, H.; Wei, Z.; Zhou, H. *Angew. Chem., Int. Ed.* **2012**, *51*, 10197−10197.
(15) Duncan, B.; Le, N. D. B.; Alexander, C.; Gupta, A.; Yesilbag Tonga, G.; Yazdani, M.; Landis, R. F.; Wang, L. S.; Yan, B.; Burmaoglu, S.; Li, X.; Rotello, V. M. *ACS Nano* **2017**, *11*, 5339−5343.
(16) Singh, N.; NaveenKumar, S. K.; Geethika, M.; Mugesh, G. *Angew. Chem.* **2021**, *133*, 3158−3167.
(17) Moons, J.; de Azambuja, F.; Mihailovic, J.; Kozma, K.; Smiljanic, K.; Amiri, M.; Cirkovic Velickovic, T.; Nyman, M.; Parac-Vogt, T. N. *Angew. Chem., Int. Ed.* **2020**, *59*, 9094−9101.
(18) Sun, M.; Xu, L.; Qu, A.; Zhao, P.; Hao, T.; Ma, W.; Hao, C.; Wen, X.; Colombari, F. M.; de Moura, A. F.; Kotov, N. A.; Xu, C.; Kuang, H. *Nat. Chem.* **2018**, *10*, 821−830.
(19) Wei, H.; Gao, L.; Fan, K.; Liu, J.; He, J.; Qu, X.; Dong, S.; Wang, E.; Yan, X. *Nano Today* **2021**, *40*, 101269.
(20) Wu, J.; Wang, X.; Wang, Q.; Lou, Z.; Li, S.; Zhu, Y.; Qin, L.; Wei, H. *Chem. Soc. Rev.* **2019**, *48*, 1004−1076.
(21) Huang, Y.; Ren, J.; Qu, X. *Chem. Rev.* **2019**, *119*, 4357−4412.
(22) Liang, M.; Yan, X. *Acc. Chem. Res.* **2019**, *52*, 2190−2200.
(23) Li, Y.; Liu, J. *Mater. Horiz.* **2021**, *8*, 336−350.
(24) Gabrielli, L.; Prins, L. J.; Rastrelli, F.; Mancin, F.; Scrimin, P. *Eur. J. Org. Chem.* **2020**, *2020*, 5044−5055.
(25) Herget, K.; Hubach, P.; Pusch, S.; Deglmann, P.; Gotz, H.; Gorelik, T. E.; Gural'skiy, I.. A.; Pfitzner, F.; Link, T.; Schenk, S.; Panthofer, M.; Ksenofontov, V.; Kolb, U.; Opatz, T.; Andre, R.; Tremel, W. *Adv. Mater.* **2017**, *29*, 1603823.
(26) Zandieh, M.; Liu, J. *ACS Nano* **2021**, *15*, 15645−15655.
(27) Breslow, R. *Artificial Enzymes*; Wiley-VCH, 2005.
(28) Li, Z.-H.; Chen, Y.; Sun, Y.; Zhang, X.-Z. *ACS Nano* **2021**, *15*, 5189−5200.
(29) Wang, X.; Lv, W.; Wu, J.; Li, H.; Li, F. *Chem. Commun.* **2020**, *56*, 4571−4574.
(30) Wang, X.; Qin, L.; Lin, M.; Xing, H.; Wei, H. *Anal. Chem.* **2019**, *91*, 10648−10656.
(31) Kim, M. S.; Lee, J.; Kim, H. S.; Cho, A.; Shim, K. H.; Le, T. N.; An, S. S. A.; Han, J. W.; Kim, M. I.; Lee, J. *Adv. Funct. Mater.* **2020**, *30*, 1905410.
(32) Xi, Z.; Wei, K.; Wang, Q.; Kim, M. J.; Sun, S.; Fung, V.; Xia, X. *J. Am. Chem. Soc.* **2021**, *143*, 2660−2664.
(33) Ji, S.; Jiang, B.; Hao, H.; Chen, Y.; Dong, J.; Mao, Y.; Zhang, Z.; Gao, R.; Chen, W.; Zhang, R.; Liang, Q.; Li, H.; Liu, S.; Wang, Y.; Zhang, Q.; Gu, L.; Duan, D.; Liang, M.; Wang, D.; Yan, X.; Li, Y. *Nat. Catal.* **2021**, *4*, 407−417.
(34) Wang, X.; Gao, X. J.; Qin, L.; Wang, C.; Song, L.; Zhou, Y. N.; Zhu, G.; Cao, W.; Lin, S.; Zhou, L.; Wang, K.; Zhang, H.; Jin, Z.; Wang, P.; Gao, X.; Wei, H. *Nat. Commun.* **2019**, *10*, 704.
(35) Shen, X.; Wang, Z.; Gao, X.; Zhao, Y. *ACS Catal.* **2020**, *10*, 12657−12665.
(36) Xu, W.; Jiao, L.; Wu, Y.; Hu, L.; Gu, W.; Zhu, C. *Adv. Mater.* **2021**, *33*, 2005172.
(37) Cheng, H. J.; Zhang, L.; He, J.; Guo, W. J.; Zhou, Z. Y.; Zhang, X. J.; Nie, S. M.; Wei, H. *Anal. Chem.* **2016**, *88*, 5489−5497.
(38) Hu, Y. H.; Cheng, H. J.; Zhao, X. Z.; Wu, J. J. X.; Muhammad, F.; Lin, S. C.; He, J.; Zhou, L. Q.; Zhang, C. P.; Deng, Y.; Wang, P.; Zhou, Z. Y.; Nie, S. M.; Wei, H. *ACS Nano* **2017**, *11*, 5558−5566.
(39) Wang, Q.; Zhang, X.; Huang, L.; Zhang, Z.; Dong, S. *Angew. Chem., Int. Ed.* **2017**, *56*, 16082−16085.
(40) Wang, C.; Nie, X. G.; Shi, Y.; Zhou, Y.; Xu, J. J.; Xia, X. H.; Chen, H. Y. *ACS Nano* **2017**, *11*, 5897−5905.
(41) Li, M.; Chen, J.; Wu, W.; Fang, Y.; Dong, S. *J. Am. Chem. Soc.* **2020**, *142*, 15569−15574.
(42) Hu, Y.; Gao, X. J.; Zhu, Y.; Muhammad, F.; Tan, S.; Cao, W.; Lin, S.; Jin, Z.; Gao, X.; Wei, H. *Chem. Mater.* **2018**, *30*, 6431−6439.
(43) Zhang, Z.; Zhang, X.; Liu, B.; Liu, J. *J. Am. Chem. Soc.* **2017**, *139*, 5412−5419.

(44) Chen, L.; Chen, Y.; Zhang, Y.; Liu, Y. *Angew. Chem., Int. Ed.* **2021**, *60*, 7654−7658.
(45) Ruan, X.; Yang, Y.; Liu, W.; Ma, X.; Zhang, C.; Meng, Q.; Wang, Z.; Cui, F.; Feng, J.; Cai, F.; Yuan, Y.; Zhu, G. *ACS Cent. Sci.* **2021**, *7*, 1698−1706.
(46) Qin, L.; Wang, X.; Liu, Y.; Wei, H. *Anal. Chem.* **2018**, *90*, 9983−9989.
(47) Zhu, Y.; Wu, J.; Han, L.; Wang, X.; Li, W.; Guo, H.; Wei, H. *Anal. Chem.* **2020**, *92*, 7444−7452.
(48) Wang, X.; Qin, L.; Zhou, M.; Lou, Z.; Wei, H. *Anal. Chem.* **2018**, *90*, 11696−11702.
(49) Li, J.; Cheng, Q.; Huang, H.; Li, M.; Yan, S.; Li, Y.; Chang, Z. *Luminescence* **2020**, *35*, 321−327.
(50) Li, J.; Lu, N.; Han, S.; Li, X.; Wang, M.; Cai, M.; Tang, Z.; Zhang, M. *ACS Appl. Mater. Interfaces* **2021**, *13*, 21040−21050.
(51) Li, X.; Kong, C.; Chen, Z. *ACS Appl. Mater. Interfaces* **2019**, *11*, 9504−9509.
(52) Wang, F.; Na, N.; Ouyang, J. *Chem. Commun.* **2021**, *57*, 4520−4523.
(53) Liu, Y.; Wang, X.; Wang, Q.; Zhang, Y.; Liu, Q.; Liu, S.; Li, S.; Du, Y.; Wei, H. *Anal. Chem.* **2021**, *93*, 15150−15158.
(54) Xu, X.; Nan, D.; Yang, H.; Pan, S.; Liu, H.; Hu, X. *Sens. Actuators, B* **2020**, *304*, 127324.
(55) Liu, Y.; Zhou, M.; Cao, W.; Wang, X.; Wang, Q.; Li, S.; Wei, H. *Anal. Chem.* **2019**, *91*, 8170−8175.
(56) Li, S.; Zhao, X.; Yu, X.; Wan, Y.; Yin, M.; Zhang, W.; Cao, B.; Wang, H. *Anal. Chem.* **2019**, *91*, 14737−14742.
(57) Wang, Y.; Wang, D.; Sun, L.-H.; Zhang, L.-C.; Lu, Z.-S.; Xue, P.; Wang, F.; Xia, Q.-Y.; Bao, S.-J. *Anal. Chem.* **2020**, *92*, 15927−15935.
(58) Zhang, T.; Zhang, S.; Liu, J.; Li, J.; Lu, X. *Anal. Chem.* **2020**, *92*, 3426−3433.
(59) Tian, X.; Liao, H.; Wang, M.; Feng, L.; Fu, W.; Hu, L. *Biosens. Bioelectron.* **2020**, *152*, 112027.
(60) An, P.; Rao, H.; Gao, M.; Xue, X.; Liu, X.; Lu, X.; Xue, Z. *Chem. Commun.* **2020**, *56*, 9799−9802.
(61) Chen, C.-Y.; Tan, Y. Z.; Hsieh, P.-H.; Wang, C.-M.; Shibata, H.; Maejima, K.; Wang, T.-Y.; Hiruta, Y.; Citterio, D.; Liao, W.-S. *ACS Sensors* **2020**, *5*, 1314−1324.
(62) Chen, W.; Zhang, X.; Li, J.; Chen, L.; Wang, N.; Yu, S.; Li, G.; Xiong, L.; Ju, H. *Anal. Chem.* **2020**, *92*, 2714−2721.
(63) Kim, H. Y.; Ahn, J. K.; Kim, M. I.; Park, K. S.; Park, H. G. *Electrochem. Commun.* **2019**, *99*, 5−10.
(64) Boriachek, K.; Masud, M. K.; Palma, C.; Phan, H.-P.; Yamauchi, Y.; Hossain, M. S. A.; Nguyen, N.-T.; Salomon, C.; Shiddiky, M. J. A. *Anal. Chem.* **2019**, *91*, 3827−3834.
(65) Tan, Z.; Dong, H.; Liu, Q.; Liu, H.; Zhao, P.; Wang, P.; Li, Y.; Zhang, D.; Zhao, Z.; Dong, Y. *Biosens. Bioelectron.* **2019**, *142*, 111556.
(66) Wu, J.; Lv, W.; Yang, Q.; Li, H.; Li, F. *Biosens. Bioelectron.* **2021**, *171*, 112707.
(67) Sun, D.; Lin, X.; Lu, J.; Wei, P.; Luo, Z.; Lu, X.; Chen, Z.; Zhang, L. *Biosens. Bioelectron.* **2019**, *142*, 111578.
(68) Fang, X.; Zhang, X.; Zhang, Z.; Hu, S.; Ye, F.; Zhao, S. *Chem. Commun.* **2021**, *57*, 3327−3330.
(69) Jiang, B.; Yan, L.; Zhang, J.; Zhou, M.; Shi, G.; Tian, X.; Fan, K.; Hao, C.; Yan, X. *ACS Appl. Mater. Interfaces* **2019**, *11*, 9747−9755.
(70) Khoris, I. M.; Chowdhury, A. D.; Li, T.-C.; Suzuki, T.; Park, E. Y. *Anal. Chim. Acta* **2020**, *1110*, 64−71.
(71) Zhang, L.; Qi, Z.; Zou, Y.; Zhang, J.; Xia, W.; Zhang, R.; He, Z.; Cai, X.; Lin, Y.; Duan, S.-Z.; Li, J.; Wang, L.; Lu, N.; Tang, Z. *ACS Appl. Mater. Interfaces* **2019**, *11*, 30640−30647.
(72) Huang, Y.; Liu, Y.; Shah, S.; Kim, D.; Simon-Soro, A.; Ito, T.; Hajfathalian, M.; Li, Y.; Hsu, J. C.; Nieves, L. M.; Alawi, F.; Naha, P. C.; Cormode, D. P.; Koo, H. *Biomaterials* **2021**, *268*, 120581.
(73) Weerathunge, P.; Ramanathan, R.; Torok, V. A.; Hodgson, K.; Xu, Y.; Goodacre, R.; Behera, B. K.; Bansal, V. *Anal. Chem.* **2019**, *91*, 3270−3276.
(74) Khoris, I. M.; Takemura, K.; Lee, J.; Hara, T.; Abe, F.; Suzuki, T.; Park, E. Y. *Biosens. Bioelectron.* **2019**, *126*, 425−432.
(75) Liu, D.; Ju, C.; Han, C.; Shi, R.; Chen, X.; Duan, D.; Yan, J.; Yan, X. *Biosens. Bioelectron.* **2021**, *173*, 112817.
(76) Wu, J.; Li, S.; Wei, H. *Nanoscale Horiz.* **2018**, *3*, 367−382.
(77) Fu, G.; Sanjay, S. T.; Dou, M.; Li, X. *Nanoscale* **2016**, *8*, 5422−7.
(78) Liu, Y.; Pan, M.; Wang, W.; Jiang, Q.; Wang, F.; Pang, D. W.; Liu, X. *Anal. Chem.* **2019**, *91*, 2086−2092.
(79) Zhou, W.; Hu, K.; Kwee, S.; Tang, L.; Wang, Z.; Xia, J.; Li, X. *Anal. Chem.* **2020**, *92*, 2739−2747.
(80) Zhang, P.; Sun, D.; Cho, A.; Weon, S.; Lee, S.; Lee, J.; Han, J. W.; Kim, D. P.; Choi, W. *Nat. Commun.* **2019**, *10*, 940.
(81) Zhu, X.; Sarwar, M.; Zhu, J.-J.; Zhang, C.; Kaushik, A.; Li, C.-Z. *Biosens. Bioelectron.* **2019**, *126*, 690−696.
(82) Xu, Y.; Xue, J.; Zhou, Q.; Zheng, Y.; Chen, X.; Liu, S.; Shen, Y.; Zhang, Y. *Angew. Chem., Int. Ed.* **2020**, *59*, 14498−14503.
(83) Ding, Y.; Ren, G.; Wang, G.; Lu, M.; Liu, J.; Li, K.; Lin, Y. *Anal. Chem.* **2020**, *92*, 4583−4591.
(84) Wang, C.; Wang, M.; Zhang, W.; Liu, J.; Lu, M.; Li, K.; Lin, Y. *Anal. Chem.* **2020**, *92*, 662−667.
(85) Liu, J.; Zhang, W.; Peng, M.; Ren, G.; Guan, L.; Li, K.; Lin, Y. *ACS Appl. Mater. Interfaces* **2020**, *12*, 29631−29640.
(86) Wu, H.; Liu, L.; Song, L.; Ma, M.; Gu, N.; Zhang, Y. *ACS Nano* **2019**, *13*, 14013−14023.
(87) Qian, X.; Han, X.; Yu, L.; Xu, T.; Chen, Y. *Adv. Funct. Mater.* **2020**, *30*, 1907066.
(88) Kim, J.; Cho, H. R.; Jeon, H.; Kim, D.; Song, C.; Lee, N.; Choi, S. H.; Hyeon, T. *J. Am. Chem. Soc.* **2017**, *139*, 10992−10995.
(89) Zhang, Y.; Wang, X.; Chu, C.; Zhou, Z.; Chen, B.; Pang, X.; Lin, G.; Lin, H.; Guo, Y.; Ren, E.; Lv, P.; Shi, Y.; Zheng, Q.; Yan, X.; Chen, X.; Liu, G. *Nat. Commun.* **2020**, *11*, 5421.
(90) Yang, F.; Hu, S.; Zhang, Y.; Cai, X.; Huang, Y.; Wang, F.; Wen, S.; Teng, G.; Gu, N. *Adv. Mater.* **2012**, *24*, 5205−5211.
(91) Huang, L.; Chen, J.; Gan, L.; Wang, J.; Dong, S. *Sci. Adv.* **2019**, *5*, No. eaav5490.
(92) Quan, Y.; Song, Y.; Shi, W.; Xu, Z.; Chen, J. S.; Jiang, X.; Wang, C.; Lin, W. *J. Am. Chem. Soc.* **2020**, *142*, 8602−8607.
(93) Cheng, L.; Wu, F.; Bao, H.; Li, F.; Xu, G.; Zhang, Y.; Niu, W. *Small* **2021**, *17*, No. 2104083.

https://doi.org/10.1021/acs.analchem.1c04492
Anal. Chem. 2022, 94, 312−323